

Super-opposition spiral dynamic-based fuzzy control for an inverted pendulum system

Ahmad Azwan Abdul Razak, Ahmad Nor Kasruddin Nasir, Nor Maniha Abd Ghani

Faculty of Electrical and Electronics Engineering Technology, Universiti Malaysia Pahang, Pekan, Malaysia

Article Info

Article history:

Received Mar 17, 2022

Revised Jun 10, 2022

Accepted Jul 9, 2022

Keywords:

Benchmark functions

Inverted pendulum

IT2FLC

Opposition learning

Single objective

Spiral dynamic algorithm

ABSTRACT

This paper presents a hybrid spiral dynamic algorithm with a super-opposition spiral dynamic algorithm (SOSDA) strategy. An improvement on the spiral dynamic algorithm (SDA), this method uses a concept centered on opposition-based learning, which is used to evaluate the fitness of agents at the opposite location to the current solution. The SDA is a simple-structured and deterministic type of algorithm, which also performs competitively in terms of solution accuracy. However, its deterministic characteristic means the SDA suffers premature convergence caused by the unbalanced diversification and intensification during its search procedure. Thus, the algorithm fails to achieve highly accurate solutions. It is proposed that adopting super-opposition into the SDA would enable the deterministic and random techniques to complement one another. The SOSDA was tested on four benchmark functions and compared to the original SDA. To analyze the result statistically, the Friedman and Wilcoxon tests were conducted. Furthermore, the SOSDA was applied to optimize the parameters of an interval type-2 fuzzy logic control (IT2FLC) for an inverted pendulum (IP). The statistical results produced by the SOSDA for both benchmark functions and the IP show that the proposed algorithm significantly outperformed the SDA. The SOSDA-based IT2FLC scheme also produced better IP responses than the SDA-based IT2FLC.

This is an open access article under the [CC BY-SA](https://creativecommons.org/licenses/by-sa/4.0/) license.



Corresponding Author:

Ahmad Azwan Abdul Razak

Faculty of Electrical and Electronics Engineering Technology, Universiti Malaysia Pahang

26600 Pekan, Pahang, Malaysia

Email: ahmadazwan.ar@gmail.com

1. INTRODUCTION

The spiral dynamic algorithm (SDA) is a population-based metaheuristic algorithm and was introduced in 2011 by Nasir [1]. The main course of the SDA is the application of a spiral model equation that moves all the agents in the initialized populations in spiral steps within a predefined feasible region. During this movement, the agents' movement trajectory is defined by the preset angle and radius of the spiral step. In terms of structure, the SDA is only a simple-structured algorithm and requires low computational resources to complete the whole searching process. Due to its simple structure, the SDA processes solutions at a fast convergence speed and can search a solution near the optimal location. Nonetheless, the SDA suffers premature convergence when dealing with multimodal and high-dimensional problems. This is due to the deterministic character caused by the spiral step strategy. This defect leads the algorithm to produce a local optimum solution that is low in accuracy. The local optimum solution is not preferable as it is the result of insufficient exploration and exploitation of the searching agents. In fact, a global optimum solution is required that is produced by an algorithm and represented by a smaller value of fitness. In recent years, several studies have addressed the SDA, including modifying its structure to improve it, hybridizing the SDA

with other algorithms to increase its efficiency, and applying it in engineering problems. These studies involved the modification of the SDA using a chaotic map [2], the hybridization of the SDA with the artificial bee colony (ABC) algorithm [3], and the application of the SDA to solve mixed-integer nonlinear programming problems [4]. The studies all demonstrated successful improvements to the SDA. In other words, they showed that the SDA solved problems with better performance at a significant level.

Since the introduction of opposition-based learning (OBL) in 2004, it has been widely used in many studies, especially explorations of machine learning and metaheuristic algorithms [5]. OBL is commonly applied to improve optimization algorithms such as the genetic algorithm (GA) [6], the simulated annealing algorithm (SAA) [7], differential evolutionary (DE) [8], and particle swarm optimization (PSO) [9]. A significant study involved opposite differential evolutionary (ODE) [10]. In the work, ODE applied two generation strategies with opposite solution candidates: 1) opposite-population initialization and 2) opposite-generation jumping. ODE was evaluated using nine benchmark functions and it was proven that it performed better at a significant level. In another work, OBL was adopted into the GA, which became known as the opposition GA (OGA) [11]. This approach applied a standard opposition to produce anti-chromosomes for the best and worst agents in a population. In another study, the OBL scheme was adopted into PSO to form opposition-based PSO (O-PSO) [12]. O-PSO only used OBL to initialize the opposition population in the early phase. Meanwhile, many other algorithms can be found in the literature that take advantage of OBL, including opposition-based harmony search (OHS) [13], opposition-based PSO with velocity clamping (OVCP SO) [14], enhanced-opposition-based PSO (EOPSO) [15], and the opposition-based memetic algorithm (OBMA) [16]. These studies concluded that OBL successfully improved the algorithms by increasing the convergence curve while also improving the accuracy of the final solution.

Based on motivation of *no free lunch theorem*, a theoretical knowledge finds that optimization algorithms perform equally good based on the mean of their performance across all possible landscapes of objective function. The theorem also defines that, algorithms could perform well and worst in certain problems, which mean that if an algorithm performed well in a problem, it does not mean that the algorithm will perform well in all existing problems. This paper, a variant of the SDA based on OBL is proposed, namely the super-opposition spiral dynamic algorithm (SOSDA). It adopted super opposition-based learning to improve agent spread during the searching process. Thus, the diversification and intensification of the algorithm are improved, which leads to a global optimum location. The proposed SOSDA is used to optimize the control scheme of an inverted pendulum (IP) system [17]. In the work, an interval type-2 fuzzy logic controller (IT2FLC) was chosen to stabilize the movement of the IP cart while maintaining the upright position of the pendulum [18]. The paper is organized as follows: section 2 presents the description and corresponding parameters of the IP, while section 3 elaborates the SDA and SOSDA in detail. Section 4 presents the experimental setup for the benchmark functions test and the setup for the IT2FLC. In section 5, the results of the SOSDA performance in relation to the benchmark function and application are presented, while section 6 concludes the work of the SOSDA.

An inverted pendulum is an unstable and underactuated nonlinear system [17]. Figure 1 presents a schematic diagram of the IP used in this work. The IP is a machine that is widely used for testing a new control scheme. It consists of a freely rotating pole attached to a cart's body, which moves back and forth in translational movement. In stationary conditions, the pendulum points downward. In contrast, the IP is operated by moving the cart from its original position to a desired position. The cart forces the pivoted pole to rotate freely around its axis to reach a final pendulum state in which it is pointing vertically upward. The IP is a one-input many-output, in which a voltage signal is considered to be the input, while the cart's position and the pole's position are considered to be the outputs [18]. Generally, the objective of a control scheme is to regulate the cart's movement while maintaining the upright position of the pendulum. In terms of the application similarities, the IP represents two-wheel Segway transporters [19], two-wheeled chairs for disabled persons [20], and space rockets [21]. The physical parameters for the IP are shown in Table 1. The figure and table illustrate that the derivation of the system can be based on Newton's second law of motion [22]. The expressions were derived and are simplified in (1)–(8). Meanwhile, F_r and F_v in the equations is expressed in (1)–(3).

$$(M + m)\ddot{x} + ml\ddot{\theta} + F_r\dot{x} = F_vV \quad (1)$$

$$F_r = b + (2\pi/r)^2 (K_m K_b / R) \quad (2)$$

$$F_v = (2\pi K_m) / rR \quad (3)$$

Where b is the coefficient of friction, r is the length of the transfer per-revolution of the ball-screw, K_m is the torque constant, K_b is the back-emf constant, and R is the armature resistance of the motor. The differential equation for the pendulum was derived, as shown in (4).

$$m\ddot{x} + ml\ddot{\theta} = mg\theta \quad (4)$$

Furthermore, the previous equations of motion were converted to state-space equations, as shown in (5)-(6).

$$\begin{bmatrix} \dot{x}_1 \\ \dot{x}_2 \\ \dot{x}_3 \\ \dot{x}_4 \end{bmatrix} = \begin{bmatrix} 0 & 1 & 0 & 0 \\ \frac{(M+m)g}{Ml} & 0 & 0 & \frac{F_r}{Ml} \\ 0 & 0 & 0 & 1 \\ -\frac{mg}{M} & 0 & 0 & -\frac{F_r}{m} \end{bmatrix} \begin{bmatrix} x_1 \\ x_2 \\ x_3 \\ x_4 \end{bmatrix} + \begin{bmatrix} 0 \\ -\frac{F_V}{Ml} \\ 0 \\ \frac{F_V}{M} \end{bmatrix} u \tag{5}$$

$$y = \begin{bmatrix} 1 & 0 & 0 & 0 \\ 0 & 0 & 1 & 0 \end{bmatrix} \begin{bmatrix} x_1 \\ x_2 \\ x_3 \\ x_4 \end{bmatrix} \tag{6}$$

The values in Table 1 were then substituted into (5) to (6) and formed by following (7) and (8) to become the final derivation from the whole system using state-space equations.

$$\begin{bmatrix} \dot{x}_1 \\ \dot{x}_2 \\ \dot{x}_3 \\ \dot{x}_4 \end{bmatrix} = \begin{bmatrix} 0 & 1 & 0 & 0 \\ 29.4200 & 0 & 0 & 0.3090 \\ 0 & 0 & 0 & 1 \\ -196.1330 & 0 & 0 & -12.3615 \end{bmatrix} \begin{bmatrix} x_1 \\ x_2 \\ x_3 \\ x_4 \end{bmatrix} + \begin{bmatrix} 0 \\ -1.2121 \\ 0 \\ 48.4844 \end{bmatrix} u \tag{7}$$

$$y = \begin{bmatrix} 1 & 0 & 0 & 0 \\ 0 & 0 & 1 & 0 \end{bmatrix} \begin{bmatrix} x_1 \\ x_2 \\ x_3 \\ x_4 \end{bmatrix} \tag{8}$$

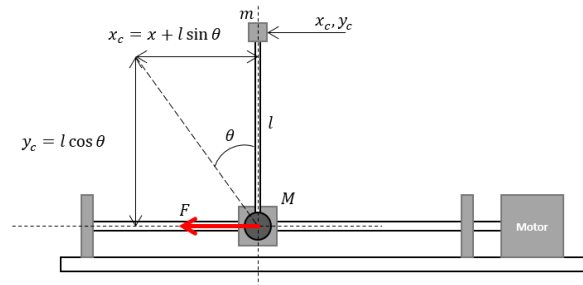


Figure 1. Free-body diagram of cart-pendulum system

Table 1. Parameter values of the inverted pendulum system

Parameter	Values
Mass of cart, M	0.1 kg
Mass of pendulum, m	0.05 kg
Friction of cart, b	$0.1 \text{ Nm}^{-1} \text{ s}^{-1}$
Length of pendulum, l	0.3 m
Motor torque constant, K_m	4.9 Ncm A^{-1}
Motor back emf constant, K_b	$0.0507 \text{ V rad}^{-1} \text{ s}^{-1}$
Motor armature resistant, R	0.3 Ω

2. PROPOSED SUPER OPPOSITION-SPIRAL DYNAMIC ALGORITHM

The proposed SOSDA involves coaction between the Super-opposition type of OBL and the SDA. The addition of super-opposition OBL into the SDA led to a higher chance of producing an optimal solution as it helped the algorithm to generate and evaluate the agents at the opposite location. As the SDA diverges in the initial phase and concentrates in the end phase, unbalanced exploration and exploitation occur. It is important to make the agents spread well throughout the process from the beginning to the end to improve chances of producing a global solution. Thus, the addition of Super-opposition into the SDA improved the algorithm's ability to both explore and exploit. The super-opposition formula used in this work is presented as (9).

$$\hat{x}_{SO} = (a + b - \hat{x}) + rand(2b - a + \hat{x}) \tag{9}$$

Where a and b are the lower and upper boundaries for a specific problem, x is the current location of the agents, and $rand$ is a random number between $[0,1]$. Conversely, the SDA is an optimization algorithm that

is also categorized as a population-based optimization algorithm. It implements a spiral model to move all the agents from one point to another. The spiral model can be mathematically expressed as (10):

$$x_i^d(k + 1) = S_n(r, \theta)x_i^d(k) - S_n(r, \theta) - I_n\hat{x}^*, i = 1, 2, 3, \dots, m \tag{10}$$

where $x_i(k + 1)$ is the new location of the i^{th} searching agent in a certain d^{th} dimension of D , while in the k^{th} iteration, this is the previous location of the i^{th} searching agent, I is the identity square matrix, r and θ represent the spiral radius and angle respectively. $S(r, \theta)$ is the rotation matrix defined in terms of r and θ , while x^* is the spiral center point. Note that x^* is also the best solution found so far and might be the best solution after all the iteration has completed.

Algorithm 1. Pseudocode of the SOSDA

```

Input data:  $r, \theta, k_{max}, D, m$ 
Initialize a population ( $pop$ ) consisting of agents  $x_i$  with a number of  $m$  agents.
Generate a population of opposite agents,  $pop_{opp}$  based on  $pop$  using (9).
Compute the fitness value of each agent  $f_i = f(x_i)$  and their opposite,  $f_{opp_i} = f(x_{opp_i})$ 
Choose only the  $m$  fittest particles, and the first ranked particles is the center,  $x^*$ 
Set  $k = 1$ 
While ( $k < k_{max}$ )
    For  $i = 1:m$ 
        Apply the spiral model equation using (10).
        Generate opposition,  $x_{i_{opp}}$  using (9).
    End For
    Calculate the fitness of the agents.
    Update the center,  $x^*$ 
    Choose only  $m$  of the fittest particles.
Update  $k = k + 1$ 
End While
Return  $x_{best}$ 

```

3. METHOD

3.1. Benchmark functions

In the current work, four different test functions were utilized to examine the accuracy of the proposed algorithm’s performance [22]. The mathematical expressions of the test functions are expressed in Table 2. Functions 1 to 4 are the rotated high conditioned elliptic function, shifted, and rotated Rosebrock’s function, hybrid function 1 (N=3), and composition function 1 (N=5), respectively. All these functions were selected from different categories and landscapes of problems. This was to prove that the proposed algorithm would produce better solutions for different kinds of problems. The functions were tested on 100 dimensions and the search range was defined as [-100,100]. For a fair analysis and comparison of the results, 51 total runs were conducted for each benchmark function [23].

Table 2. Formula of each benchmark function

	Num.	
Unimodal Functions	1	$f_1(x) = \sum_{i=1}^D (10^6)^{\frac{i-1}{D-1}} x_i^2$
Simple Multimodal Functions	2	$f_2(x) = \sum_{i=1}^{D-1} (100(x_i^2 - x_{i+1})^2 + (x_i - 1))$ $N = 3$ $p = [0.3, 0.3, 0.4]$
Hybrid Function [22]	3	$g1$: Modified Schwefel's $g2$: Rastrigin's $g3$: High Conditioned Elliptic $N = 5$, $\sigma = [10, 20, 30, 40, 50]$ $\lambda = [1, 1e-6, 1e-26, 1e-6, 1e-6]$ $bias = [0, 100, 200, 300, 400]$
Composition Functions [22]	4	$g1$: Rotated Rosenbrock's $g2$: High Conditioned Elliptic $g3$ Rotated Bent Cigar $g4$: Rotated Discus $g5$: High Conditioned Elliptic

3.2. IT2FLC of the inverted pendulum system

The T2FL model is the continuation of an ordinary fuzzy logic model, also called a type-1 fuzzy logic (T1FL) model [24]. The main difference between the fuzzy logic models is the fuzzy set. T1FL acquires only a single membership function, while T2FL consists of two membership functions, which appear as minimum and maximum membership functions [25]. In practical terms, these membership functions represent, respectively, the lower and upper boundaries of the type-2 fuzzy set. Furthermore, they also define the primary and secondary membership functions. The area between the lower and upper boundaries is known as the uncertainty region or the foot of uncertainties (delta). This feature enables T2FL to handle uncertainty better than T1FL. In addition, T2FL undergoes a more advanced defuzzification process. This requires a type-reducer, which transforms the inference output of type-2 to a type-1 fuzzy set before the crisp output can be computed using a defuzzifier. Figure 2 presents the block diagram of T2FLC.

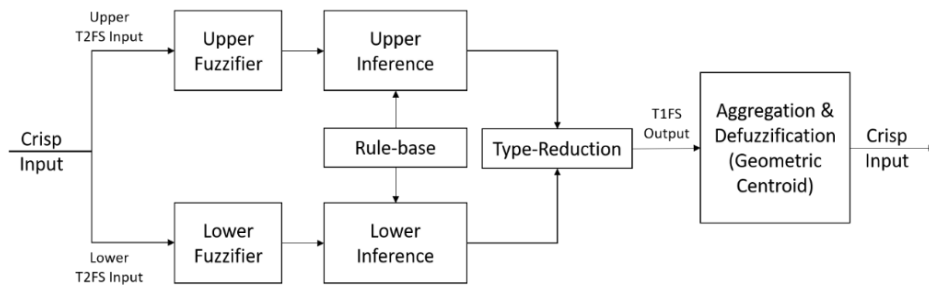


Figure 2. An interval IT2FLC consisting of separate fuzzifiers for the lower and upper type-2 fuzzy set inputs

To determine the accuracy performance of the opposition-spiral algorithm, a control scheme involving T2FL was designed. In the study, T2FL (IT2FL) was implemented with the IP. The control scheme block diagram is illustrated in Figure 3. The focus of interest is the position of the cart ($d=10$ cm) while the pendulum points upward. The responses produced from the movement were the outputs, which were compared against the desired cart position input. As the outcome, the difference between the cart's actual and desired positions is the IT2FL input. Furthermore, the SDA and proposed SOSDA were used in the searching process to minimize the error. Thus, a set of optimized parameters consisting of rules and gains for the IT2FL control could be determined. The objective of the presented optimization algorithm was to remove the error of the angular position of the pendulum in the vertical position while positioning the cart in the desired position at a certain distance from the center of horizontal. The fitness cost known as root mean square error (RMSE) was used in this work and the expression is stated in (11).

$$RMSE = \sqrt{\frac{1}{N} \sum_{i=1}^N (e^2)} \tag{11}$$

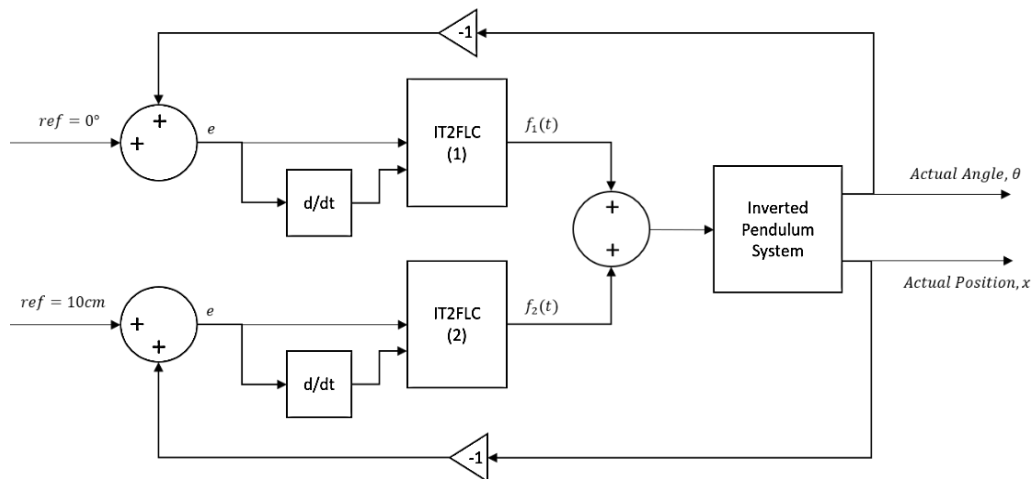


Figure 3. Block diagram of the control scheme for the inverted pendulum system

RMSE was used as part of the fitness function, whereas the summation of the RMSE of the cart's position and the pendulum's angle were acquired by taking the weightage of the two desired objectives by $[w_1 \ w_2] = [0.5 \ 0.5]$. Note that w_1 is the cart position weightage and w_2 is the weightage of the pendulum's angle. These weightage values were chosen due to the similar priority of the objective to achieve the correct cart position while the angle of the pendulum placed it in an upright position. The fitness function for the system is shown as (12).

$$\text{Fitness} = w_1 RMSE_1 + w_2 RMSE_2 \quad (12)$$

In (12), $RMSE_1$ and $RMSE_2$ represent the error of the cart's position and the angular position of the pendulum, respectively.

4. RESULTS AND DISCUSSION

4.1. Benchmark functions test

This section presents the performance analysis of the SDA and the proposed SOSDA on four different landscapes of the benchmark problems. The observations from the performance tests were analyzed using numerical analysis tools. In the work, the Wilcoxon signed-rank test was used to determine the significant level of improvement [26]. Table 3 displays the mean values of the accuracy performance acquired from 51 independent runs. The table concludes that the new variant algorithm provided more accurate solutions compared to the SDA.

Table 3. Mean accuracy produced by each algorithm

Function	Mean accuracy	
	SDA	SOSDA
1	3.03E+09	1.18E+09
2	5.42E+04	1.49E+04
3	3.27E+08	1.18E+08
4	4.06E+03	3.21E+03

The results outlined in Table 3 were further evaluated using the Wilcoxon signed-rank test. The purpose of using this tool is to determine the contrast between the two algorithms. This study set a 5% confidence interval, so if a p -value is lower than 0.05 or 5%, the value represents a significant improvement. The results of this test are presented in Table 4. As the table shows, all the p -values are less than 0.05, while the Z -values show positive signs for all the benchmark problems. Thus, this evidence shows that the SOSDA has provided more accurate solutions. Based on the test, it can be stated that the SOSDA is a considerable improvement and can provide better solutions at a significant level of improvement.

Table 4. Wilcoxon test results

Function	Wilcoxon results	
	p -value	Z -value
1	7.739 E-09	5.774
2	7.798 E-10	6.149
3	7.340 E-5	3.965
4	5.145E-10	6.215

4.2. IT2FL control of inverted pendulum system

Other than the performance tests using benchmark functions, the presented algorithms were also applied to optimize the rules and gains for IT2FL of the IP. The study involved a total of 13 parameters (nine rules; four gains) that were to be defined. Figure 4 shows the convergence graph of the SDA and SOSDA for optimizing the required parameters of the control scheme. The figure illustrates that the SDA was trapped in local optima (3.08645) while the SOSDA continued to converge until (2.70122). This indicates that the synergy between the SDA and the super-opposition significantly improved the accuracy performance compared to the sole mechanism of the SDA.

The optimized parameters used for the IP-produced cart positioning and pendulum response are illustrated in Figures 5(a) and (b). Based on the graphical representation of the response in Figure 5(a), a slight difference was noted between the cart positions, in which the cart positioning based on the SOSDA

parameters was more accurate compared to those of the SDA. This cart positioning was achieved while the pendulum angle was in an upright position, as shown in Figure 5(b). As can be noted in the figure, the torque produced by the voltage supply optimized to the motor was stable, which resulted in the pendulum oscillating with less of an angle. Furthermore, the stability it achieved was even better than could be optimized by the SDA. The analysis of the actual cart position is displayed in Table 5. The response produced by the SOSDA had better settling and rising times than those optimized by the SDA.

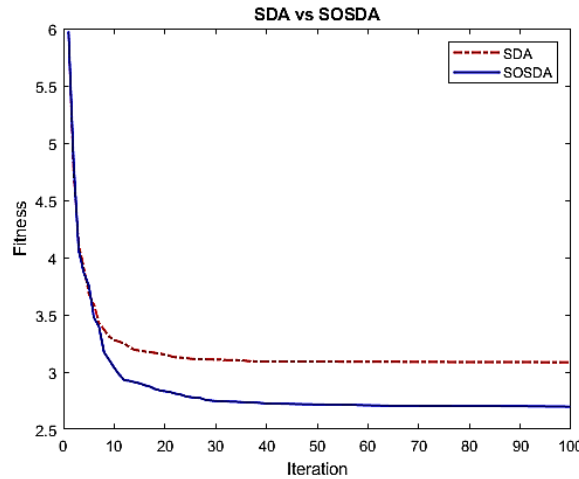


Figure 4. Convergence curve produced by the competing algorithms for the IP control scheme

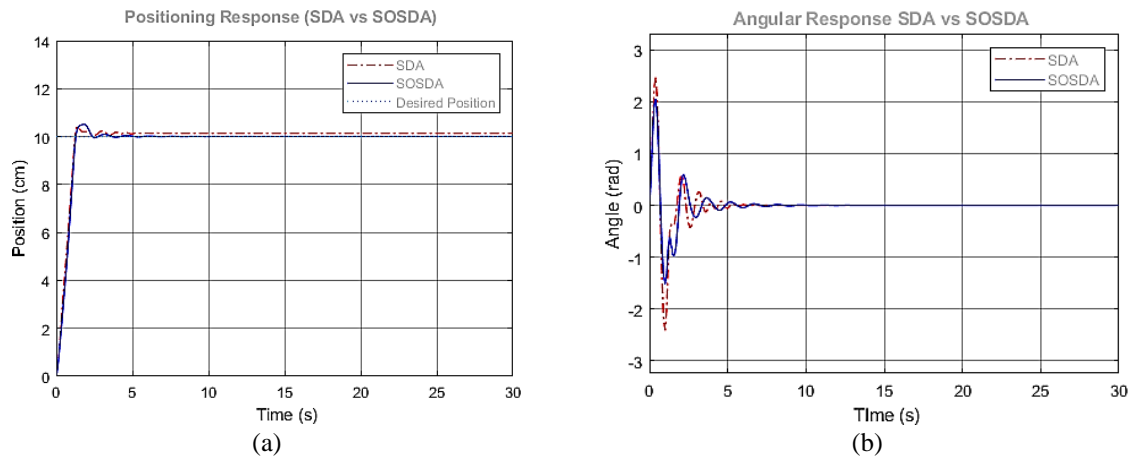


Figure 5. The response produced by the optimized parameters for (a) cart positioning at 10 cm and (b) pendulum angle

Table 5. Time response analysis of the cart performance

Parameter	Algorithm	
	SDA	SOSDA
Settling time, t_{sett}	3.7	2.7
Rise time, t_{rise}	0.744	0.771
Overshoot, % OV	13.77	0.41
Steady state error, e_{ss}	0.1377	0.0041

5. CONCLUSION

In conclusion, a new SDA variant based on OBL, called super-opposition-based learning, has been presented in this paper. This variant, called the SOSDA, can avoid premature convergence, which occurs in the SDA. Premature convergence occurs due to the insufficient exploration of the agents, whereby the agents become stuck in local optima. The synergy with super-opposition and the SOSDA created more solution

considerations as the OBL generated new agents in the opposite location. Moreover, super-opposition also improves the distribution diversity throughout the searching process. To determine the performance of the variant, four benchmark functions were chosen based on different landscapes of problems.

The test outcomes show that the SOSDA produced more accurate solutions, which was proven using the Wilcoxon signed-rank test. From the test, the proposed algorithm has satisfied the 5% confidence interval and proved that it has improved SDA significantly. The algorithms can also be applied to solve various real-world problems. In this study, the SDA and SOSDA were used to determine the best rules and gains for IT2FL controlling the IP. From the results, both the SDA and SOSDA provide good control parameters for the IT2FL and produce good cart positioning and angle control for the IP. Nonetheless, the parameters provided by the SOSDA proved slightly better in terms of rise and settling times. Thus, after these applications of the SOSDA to the benchmark functions and the IT2FL of the IP, it was concluded that the SOSDA is a promising and potential algorithm to use for SIMO-type problems. Despite of the promising feature, the computation cost of the proposed algorithm might be increased if the opposition individuals are not regulated by every loop. In particular, SOSDA is slightly increased in computation cost even the initial number of individuals was cut into half. The increasing time cost is due to the addition of time taken to generate opposition individuals for every generation of the population. In the future, the SOSDA will be modified to make it able in generating opposition individuals adaptively and planned to be adopted to solve more complex engineering problems and to optimize parameters of a neural network structure for the IP.

ACKNOWLEDGMENTS

This work has been funded by the Fundamental Research Grant Schemes FRGS/1/2019/ICT02/UMP/02/10 and FRGS/1/2019/ICT05/UMP/03/1. The fundings have been awarded by the Ministry of Higher Education Malaysia (MOHE) via the Research and Innovation Department, UMP. The university reference numbers for the grants are RDU1901196 and RDU1901217.





REFERENCES

- [1] A. N. K. Nasir, A. A. Razak, R. M. Ismail, and M. A. Ahmad, "A hybrid spiral-genetic algorithm for global optimization," *Journal of Telecommunication, Electronic and Computer Engineering (JTEC)*, vol. 10, no. 1-3, pp 93-97, 2018.
- [2] M. R. Hashim and M. O. Tokhi, "Chaotic spiral dynamics optimization algorithm," in *Advances in Cooperative Robotics*, pp. 551-558, 2016, doi: 10.1142/9789813149137_0065.
- [3] M. R. Hashim, "Improved spiral dynamics and artificial bee colony algorithms with application to engineering problems," Ph.D diss., University of Sheffield, 2018.
- [4] A. Kania and K. A. Sidarto, "Solving mixed integer nonlinear programming problems using spiral dynamics optimization algorithm," in *AIP Conference Proceedings*, vol. 1716, no. 1, p. 020004, 2016, doi: 10.1063/1.4942987.
- [5] H. R. Tizhoosh, "Opposition-based learning: a new scheme for machine intelligence," in *International conference on computational intelligence for modelling, control and automation and international conference on intelligent agents, web technologies and internet commerce (CIMCA-IAWTIC'06)*, vol. 1, pp. 695-701, 2005.
- [6] S. Mirjalili, "Genetic algorithm," *Evolutionary algorithms and neural networks*, pp. 43-55, 2019, doi: 10.1007/978-3-319-93025-1_4.
- [7] R. A. Rutenbar, "Simulated annealing algorithms: an overview," in *IEEE Circuits and Devices Magazine*, vol. 5, no. 1, pp. 19-26, Jan. 1989, doi: 10.1109/101.17235.
- [8] K. V. Price, "Differential evolution," in *Handbook of optimization*, vol. 38. pp. 187-214, 2013, doi: 10.1007/978-3-642-30504-7_8.
- [9] J. Kennedy and R. Eberhart, "Particle swarm optimization," *Proceedings of ICNN'95-International Conference on Neural Networks*, vol. 4, pp. 1942-1948, 1995, doi: 10.1109/ICNN.1995.488968.
- [10] S. Rahnamayan, H. R. Tizhoosh, and M. M. A. Salama, "Opposition-based differential evolution," in *IEEE Transactions on Evolutionary Computation*, vol. 12, no. 1, pp. 64-79, Feb. 2008, doi: 10.1109/TEVC.2007.894200.
- [11] Y. Wen, L. Liu, Z. Wang, and J. Kou, "Multi-UCAVs targets assignment using opposition-based genetic algorithm," *The 27th Chinese Control and Decision Conference (2015 CCDC)*, 2015, pp. 6026-6030, doi: 10.1109/CCDC.2015.7161891.
- [12] H. Jabeen, Z. Jalil, and A. R. Baig, "Opposition based initialization in particle swarm optimization (O-PSO)," in *Proceedings of the 11th Annual Conference Companion on Genetic and Evolutionary Computation Conference: Late Breaking Papers*, pp. 2047-2052, Jul. 2009, doi: 10.1145/1570256.1570274.
- [13] A. Banerjee, V. Mukherjee, and S. P. Ghoshal, "An opposition-based harmony search algorithm for engineering optimization problems," *Ain Shams Engineering Journal*, vol. 5, no. 1, pp. 85-101, Mar. 2014, doi: 10.1016/j.asej.2013.06.002.
- [14] F. Shahzad, A. R. Baig, S. Masood, M. Kamran, and N. Naveed, "Opposition-based particle swarm optimization with velocity clamping (OVCPSO)," in *Advances in Computational Intelligence*, vol. 116, pp. 339-348, 2009, doi: 10.1007/978-3-642-03156-4_34.
- [15] J. Tang and X. Zhao, "An enhanced opposition-based particle swarm optimization," *2009 WRI Global Congress on Intelligent Systems*, 2009, pp. 149-153, doi: 10.1109/GCIS.2009.56.
- [16] Q. Zhou, U. Benlic, and Q. Wu, "An opposition-based memetic algorithm for the maximum quasi-clique problem," *European Journal of Operational Research*, vol. 286, no. 1, pp. 63-83, Oct. 2020, doi: 10.1016/j.ejor.2020.03.019.
- [17] A. A. A. Razak, A. N. K. bin Nasir, N. M. A. Ghani, S. Mohammad, M. F. M. Jusof, and N. A. M. Rizal, "Hybrid genetic manta ray foraging optimization and its application to interval type 2 Fuzzy logic control of an inverted pendulum system," in *IOP Conference series: materials science and engineering*, vol. 917, no. 1, p. 012082, 2020.
- [18] S. M. Abuelenin, "Decomposed interval type-2 fuzzy systems with application to inverted pendulum," *2014 International*





- Conference on Engineering and Technology (ICET)*, 2014, pp. 1-5, doi: 10.1109/ICEngTechnol.2014.7016752.
- [19] M. Sharma, R. Sharma, K. Singh, V. Sinha, and S. Tadavi, "Segway—the human transporter," *IJIRST—International Journal for Innovative Research in Science & Technology*, vol. 1, no. 1, pp. 128-132, Apr. 2015.
- [20] N. M. A. Ghani and M. O. Tokhi, "A dwi-phase fuzzy control structure for an auto-mode stair climbing wheelchair," *2013 IEEE International Conference on Systems, Man, and Cybernetics*, 2013, pp. 4694-4699, doi: 10.1109/SMC.2013.799.
- [21] R. Daines, Russell and C. Segal, "Combined rocket and airbreathing propulsion systems for space-launch applications," *Journal of Propulsion and Power*, vol. 14, no. 5, pp. 605-612, 1998, doi: 10.2514/2.5352.
- [22] J. J. Liang, B. Y. Qu, and P. N. Suganthan, "Problem definitions and evaluation criteria for the CEC 2014 special session and competition on single objective real-parameter numerical optimization," *Computational Intelligence Laboratory, Zhengzhou University, Zhengzhou China and Technical Report, Nanyang Technological University, Singapore*, vol. 635, p. 490, 2014.
- [23] A. Azwan, A. Razak, M. F. M. Jusof, A. N. K. Nasir, and M. A. Ahmad, "A multiobjective simulated Kalman filter optimization algorithm," *2018 IEEE International Conference on Applied System Invention (ICASI)*, 2018, pp. 23-26, doi: 10.1109/ICASI.2018.8394257.
- [24] H. A. Al-Jamimi and T. A. Saleh, "Transparent predictive modelling of catalytic hydrodesulfurization using an interval type-2 fuzzy logic," *Journal of cleaner production*, vol. 231, pp. 1079-1088, Sep. 2019, doi: 10.1016/j.jclepro.2019.05.224.
- [25] M. F. Masrom, N. M. A. Ghani, and M. O. Tokhi, "Particle swarm optimization and spiral dynamic algorithm-based interval type-2 fuzzy logic control of triple-link inverted pendulum system: A comparative assessment," *Journal of Low Frequency Noise, Vibration and Active Control*, vol. 40, no. 1, pp. 367-382, 2021, doi: 10.1177/1461348419873780.
- [26] S. M. Taheri and G. Hesamian, "A generalization of the Wilcoxon signed-rank test and its applications," *Statistical Papers*, vol. 54, no. 2, pp. 457-470, 2013, doi: 10.1007/s00362-012-0443-4.

BIOGRAPHIES OF AUTHORS







Ahmad Azwan bin Abdul Razak     received a Bachelor (Hon.) of Mechatronics Engineering from Universiti Malaysia Pahang, as well as also received Bachelor of Engin. from Karlsruhe University of Applied Science in 2016. He received a Master of Science degree in Electronic Engineering (majoring in control system and system optimization). Currently, he is a Research assistant at the Faculty of Electrical and Electronics Engineering Technology, Universiti Malaysia Pahang. His research interests include developing optimization algorithms and their application in artificial and real-world problems, artificial intelligent, and control system. He can be contacted at email: ahmadazwan.ar@gmail.com.



Ahmad Nor Kasruddin Nasir     is an Associate Professor at the Faculty of Electrical and Electronics Engineering Technology, Universiti Malaysia Pahang, Malaysia. He has been the faculty member since 2005. He received a Mechatronics Engineering degree from IIUM, Malaysia in 2005, and a Master Degree from Universiti Teknologi Malaysia, Malaysia in 2007. He completed his Doctoral Degree from the University of Sheffield, UK in 2014. His work interests are primarily in the field of artificial intelligence, robotics, and mechatronics as well as soft computing. He has authored and co-authored over 70 research publications. He can be contacted at email: kasruddin@ump.edu.my.



Nor Maniha Abdul Ghani     is an Associate Professor who is currently at Engineering College, Universiti Malaysia Pahang. She received her Bach.Eng. and M.Eng. in 2003 and 2006 respectively from Universiti Teknologi Malaysia. She received a Ph.D. degree in 2015 from the Sheffield University, UK. Her current work interests include modelling and system design, optimization of control parameter, and intelligent control. She can be contacted at email: normaniha@ump.edu.my.